

# Calibration of Charge Detection MS Instruments

Authors: *Keith Richardson<sup>1</sup>; Kevin Giles<sup>1</sup>; Anisha Haris<sup>1</sup>; Benjamin Draper<sup>2</sup>; Martin Jarrold<sup>2</sup>*  
Affiliations: <sup>1</sup>Waters Corporation, Wilmslow, UK; <sup>2</sup>Megdalton Solutions Inc., Bloomington, IN

## OVERVIEW

### PURPOSE:

- Introduce  $m/z$  and charge calibration of a charge detection MS (CDMS) instrument.
- Develop a novel approach to  $m/z$  calibration using high-mass standards having uncertain masses.
- Quantify and propagate uncertainties in  $m/z$  following calibration.

### METHOD:

- $m/z$  calibration using a single parameter and two-parameter linear calibration of charge state.
- Specify a theoretical minimum mass for each standard.
- Adopt a Bayesian approach that explicitly acknowledges the uncertainty in the additional mass.

### RESULTS:

- We obtain  $m/z$  calibrations having precision better than 0.1% and charge precisions of significantly less than unit charge for measurements over 100 ms trapping times.

## INTRODUCTION

Charge Detection Mass Spectrometry (CDMS) has the potential to significantly extend the utility of mass spectrometry for the analysis of high molecular weight and highly heterogeneous samples. This is possible because simultaneous measurement of the mass-to-charge ratio ( $m/z$ ) and charge state ( $z$ ) of individual ions allows determination their mass, significantly reducing the complexity of electrospray MS data for these species.

We describe approaches to both  $m/z$  and  $z$  calibration, using appropriate standards and a novel algorithmic treatment in order to capture and propagate relevant uncertainties.

An unusual aspect of CDMS calibration is that, owing to their size, calibration standards can carry additional mass (e.g. residual solvent), and we explain how this can be accounted for during the calibration process.

## METHODS

The Electrostatic Linear Ion Trap CDMS (ELIT CDMS) instrument used in this study is shown in Figure 1. Oscillating ions in the trap induce a charge on the detector tube which is measured using a charge-sensitive amplifier. The design of the detection tube ensures that 100% of the ions' charge is induced onto the detector, allowing high-resolution charge measurements for each individual ion.

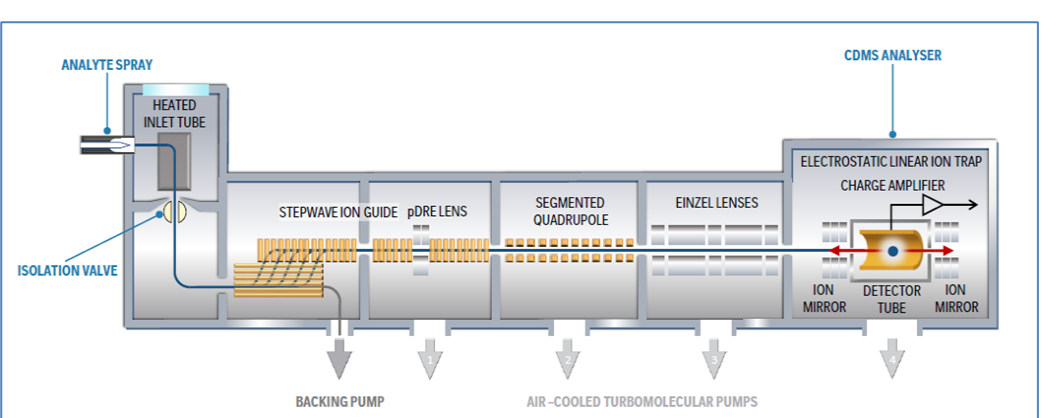


Figure 1. The Electrostatic Linear Ion Trap Charge Detection Mass Spectrometer

Waters is a trademark of Waters Technologies Corporation

Indeed for sufficiently long trapping times, the charge of individual ions can be determined exactly<sup>1</sup>. In order to do this, however, a calibration relationship must be established between the magnitude of the observed signal and the charge state of the ions.

Careful amplifier design and appropriate signal processing ensures that the magnitude  $A$  of the induced voltage is nearly proportional to each ion's charge state. In practice a linear calibration is employed to allow for (and measure) small offsets in charge measurement:

$$z = c_1 + c_2 A \quad (1)$$

These constants are determined using protein standards that can be resolved by  $m/z$  in order that a representative magnitude can be determined for each charge state.

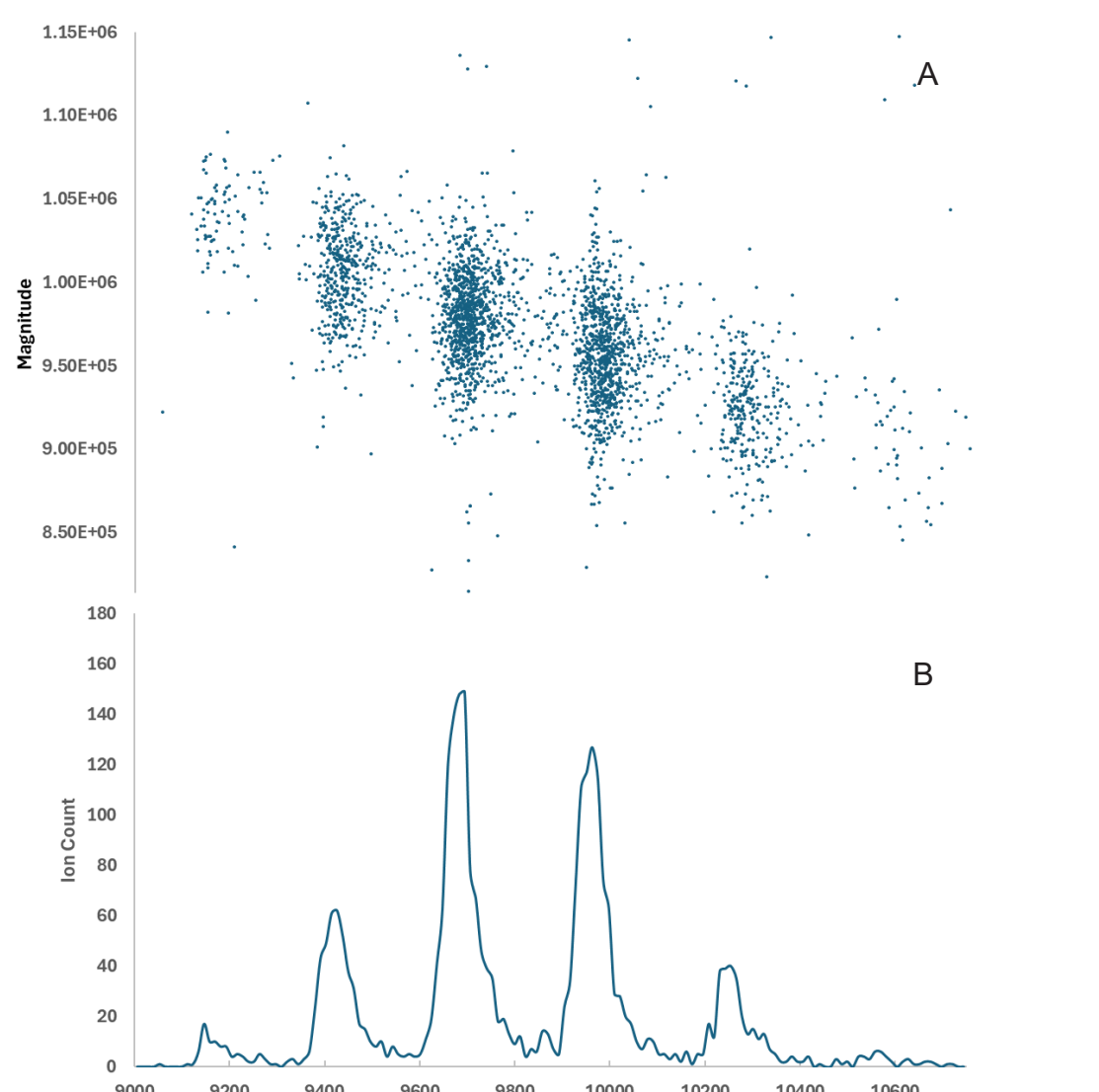


Figure 2. CDMS data corresponding to six charge states of the hexamer of L-Glutamate Dehydrogenase (GDH). A) Magnitude plotted against  $m/z$  ratio. Each dot represents a 100 ms trapping time single ion detection. B) The same data represented as a conventional  $m/z$  spectrum with a provisional calibration.

Figure 2A shows a scatter plot of individual ion detections for a protein standard with the y-axis representing signal magnitude  $A$ . Although the 100 ms trapping time employed here (charge RMSD  $\sim 0.9e$ ) does not result in baseline charge resolution ( $\sim 0.2e$ ), the gradual decrease in magnitude with  $m/z$  (decreasing charge state) is visible.

Because the charge states are resolved by  $m/z$ , a charge calibration can be formed by determining representative magnitudes corresponding to individual charge state peaks for a number of standards. Having done this, the parameters  $c_1$  and  $c_2$  in equation (1) can be determined using a straightforward linear fit. However in order to do this it is necessary to correctly assign charge states to these peaks, which requires  $m/z$  calibration.

## M/Z CALIBRATION

It is desirable to utilize calibration standards having a wide range of charge states to establish a high-quality charge calibration. The same standards can also contribute usefully to  $m/z$  calibrations. However higher mass standards can also carry a significant amount of extra mass in the form of adducts. This uncertain additional mass must be taken into account during  $m/z$  calibration.

The relationship between frequency and  $m/z$  in an electrostatic ion trap is given by

$$\frac{m}{z} = \frac{k}{F^2}$$

Where  $k$  is a constant (to be calibrated) which depends on the geometry of the trap, ion energy, and the applied voltages. The calibration dataset will typically consist of series of data for  $N$  standards having known masses  $m_1, m_2, \dots, m_N$ . Each of these standards will be represented in the data by a number of charge states  $z=z_{n1}, z_{n2}, \dots$  for the  $i$ 'th standard ( $1 \leq i \leq N$ ). We allow that each standard has some *a-priori* unknown amount of excess mass  $\delta_i$  attached which we currently assume to be the same for each charge state so that the observed  $m/z$  values  $d_{ij}$  (where  $j$  indexes charge states), obtained using a provisional calibration will be

$$d_{ij} \sim g \frac{m_i + \delta_i}{z_{ij}} \pm \sigma_{ij}$$

where  $g$  is an *a-priori* unknown scaling factor ( $g=1.0$  if the provisional calibration constant  $k$  is exactly correct). Following calibration,  $k$  will be updated to a revised value  $k'=g$ . The  $\sigma_{ij}$  are uncertainties in the  $m/z$  measurements which are obtained by peak detecting a spectrum such as that shown in Figure 2B. Note that for simplicity we have ignored the mass of charge carriers here: although relatively small these are easily included in the analysis.

We adopt a Bayesian approach, which requires that we assign prior probability distributions to the unknown parameters  $g$  and  $\delta_i$ . To avoid unnecessary complication here we assign an improper uniform prior to the calibration parameter  $g$ . Because the excess mass parameters  $\delta_i$  are known to be positive, an exponential prior for these is appropriate:

$$\Pr(\delta_i) = \frac{1}{\Lambda_i} \exp\left(-\frac{\delta_i}{\Lambda_i}\right)$$

where  $\Lambda_i$  is the expected scale of additional mass (e.g. 1% of  $m$ ). Assuming a Gaussian likelihood function, the joint probability of the data and parameters is

$$\Pr(d, \delta_1, \delta_2, \dots, g) = \prod_i \frac{1}{\Lambda_i} \exp\left(-\frac{\delta_i}{\Lambda_i}\right) \prod_{j \in z_i} \frac{1}{\sqrt{2\pi}\sigma_{ij}} \exp\left(-\frac{(d_{ij} - g \frac{m_i + \delta_i}{z_{ij}})^2}{2\sigma_{ij}^2}\right) \\ = \frac{1}{(2\pi)^{N/2}} \prod_{ij} \frac{1}{\sigma_{ij}} \prod_i \frac{1}{\Lambda_i} \exp\left(-\frac{(\delta_i - \delta_{i0})^2}{2\Lambda_i^2}\right) \exp\left(\sum_i \left(\frac{B_i^2}{4\Lambda_i} - C_i\right)\right)$$

where in the second line we have simply rearranged the expression (to facilitate marginalization) and defined the new symbols

$$A_i = \frac{1}{2}g^2 X_i \quad B_i = g^2 m_i X_i - g Y_i + \frac{1}{\Lambda_i} \\ C_i = \frac{1}{2}g^2 m_i^2 X_i - g m_i Y_i + \frac{1}{2}Z_i \quad S_i = \frac{1}{\sqrt{2\Lambda_i}} \quad \delta_{i0} = -\frac{B_i}{2\Lambda_i} \\ X_i = \sum_{j \in z_i} \frac{1}{z_j^2 \sigma_{ij}^2} \quad Y_i = \sum_{j \in z_i} \frac{d_{ij}}{z_j \sigma_{ij}^2} \quad Z_i = \sum_{j \in z_i} \frac{d_{ij}^2}{\sigma_{ij}^2}$$

Since we are not primarily interested in the additional mass parameters  $\delta_i$ , they can be "marginalized" i.e. integrated out of the full joint probability to give the joint probability of  $g$  and the data:

$$\Pr(d, g) = \int_0^\infty \int_0^\infty \Pr(d, \delta_1, \delta_2, \dots, g) d\delta_1 d\delta_2 \dots \\ \propto \exp\left(\sum_i \left(\frac{B_i^2}{4\Lambda_i} - C_i\right)\right) \prod_i S_i \left(1 + \operatorname{erf}\left(\frac{\delta_{i0}}{\sqrt{2}S_i}\right)\right) \quad (2)$$

where  $\operatorname{erf}$  is the error function. Everything in this joint probability distribution is known except  $g$ , so despite the apparent complexity it is just a 1D distribution. It is therefore straightforward to obtain samples of  $g$  to determine the required calibration scaling  $g$  together with the associated uncertainty. The posterior probability distribution  $\Pr(g|d) = \Pr(g, d)/\Pr(d)$  is obtained by normalizing with respect to  $g$  if required. The denominator  $\Pr(d)$  is the "Evidence", obtained by integrating  $\Pr(g, d)$  over  $g$  and is useful in model comparison (e.g. comparing possible charge state assignments).

We illustrate this new calibration approach using simulated data for three hypothetical high-mass calibrants as described in Table 1.

| Calibrant #                | 1      | 2      | 3      |
|----------------------------|--------|--------|--------|
| Expected Mass (kDa)        | 150    | 350    | 600    |
| Min Charge State           | 20     | 40     | 60     |
| Max Charge State           | 24     | 45     | 63     |
| Expected Excess Mass (kDa) | 0.15   | 3.5    | 6.0    |
| Simulated Mass (kDa)       | 150.04 | 353.41 | 608.89 |

Table 1. Expected masses, charge state ranges, expected excess mass and simulated masses for the three simulated calibrant species.

Simulated mass excesses for each calibrant were sampled from exponential distributions having scale factors set by the expected excess masses ( $\Lambda_i$ ) shown in the table. Simulated  $m/z$  values  $d_{ij}$  for each charge state were then sampled from Gaussian distributions with a standard deviation of 100 ppm. The simulated calibration scaling factor was  $g=1.1$ .

$\Pr(g, d)$

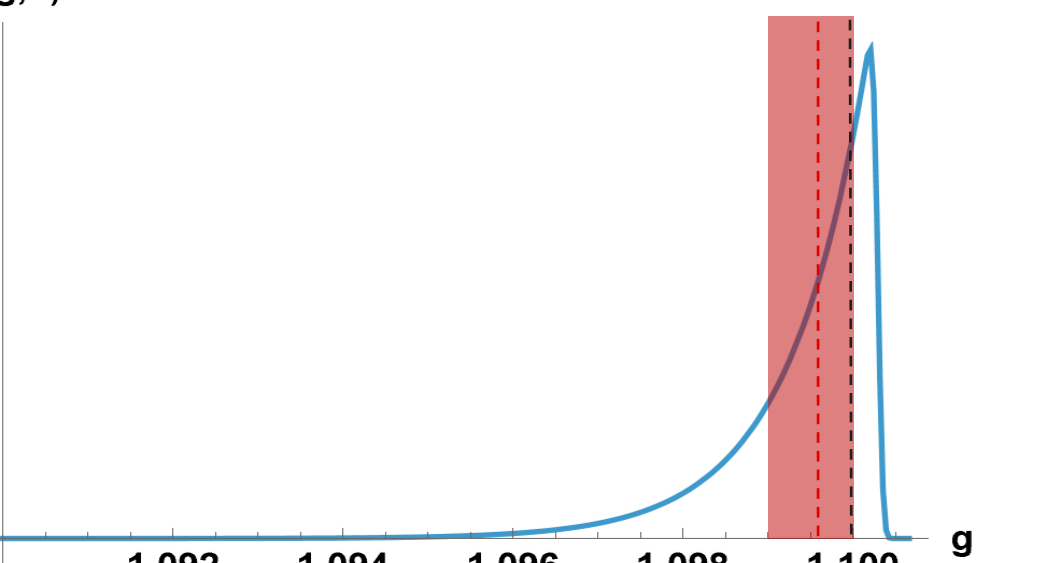


Figure 3. Probability distribution (blue) for the calibration scale parameter  $g$  and the data. The dotted red line shows the position of the median:  $g_m=1.0996$  and the shaded region is the interquartile range (Q1, Q3) = (1.0990, 1.1001). The black dotted line shows the true value  $g_t=1.1$ .

The resulting joint probability distribution  $\Pr(g, d)$  is shown in Figure 3. The most obvious feature of this is the sharply asymmetrical distribution. This correctly reflects the fact that  $g$  cannot take a value that would imply a negative value for any of the  $\delta_i$  since these are mass excesses. Because of this asymmetry, we choose to report a median and interquartile range rather than a mean and standard deviation for the distribution. The median is  $g_m=1.0996$ , which is 0.03% below the true value  $g_t=1.1$ , and the true value lies within the interquartile range.

## EXPERIMENTAL RESULTS

L-Glutamate Dehydrogenase (GDH), human serum albumin (HSA), Enolase, beta-lactoglobulin (BLG) and the Waters™ mass check mAb standard were buffer exchanged into 200 mM ammonium acetate solution using Bio-Spin® P-6 size-exclusion columns (Bio-Rad Laboratories). Ions were generated in positive ion mode using nanoelectrospray ionization and mass analysis was performed using two mechanically equivalent prototype electrostatic linear ion trap CDMS systems CDMS1 and CDMS2. At the time the calibration of the CDMS2 instrument was made, the BLG sample was not available. Signal processing and data visualization were performed using novel software developed in-house. Ions were trapped for 100 ms and the frequency and amplitude information were converted to  $m/z$  and  $z$  values respectively, and ultimately mass ( $m/z \times z$ ). Spectra were peak detected using a modified deconvolution algorithm to obtain an  $m/z$  value for each charge state of each standard. The details for each calibrant are shown in Table 2.

| Calibrant             | GDH   | HSA  | Enolase | BLG*  | mAb   |
|-----------------------|-------|------|---------|-------|-------|
| Expected Mass (kDa)   | 333.5 | 66.4 | 93.37   | 18.36 | 149.1 |
| Min Charge State      | 34    | 15   | 18      | 6     | 21    |
| Max Charge State      | 39    | 17   | 20      | 7     | 24    |
| Expected Excess (kDa) | 7     | 1    | 1       | 0.02  | 0.1   |

Table 2. Expected masses, charge state ranges, expected excess masses and simulated masses for the experimental calibrant species. \*BLG was not used in the calibration of the CDMS2 instrument.

The calibration results for the two instruments are shown in Table 3.

| Instrument                | CDMS1  | CDMS2  |
|---------------------------|--------|--------|
| Scaling Factor (g)        | 1.0314 | 1.0348 |
| Interquartile Range (ppm) | 330    | 541    |
| RMS m/z error (ppm)       | 593    | 648    |

Table 3. Inferred scale factors for instruments CDMS1 and CDMS2 with associated interquartile ranges and RMS (residual) errors expressed in parts-per-million (ppm).

Prior to calibration, the instruments had identical provisional calibrations, so it is notable that the scaling factors lie within 0.4% of each other, suggesting good reproducibility in instrument construction. The detailed  $m/z$  residuals for the CDMS1 instrument are shown in Figure 4.

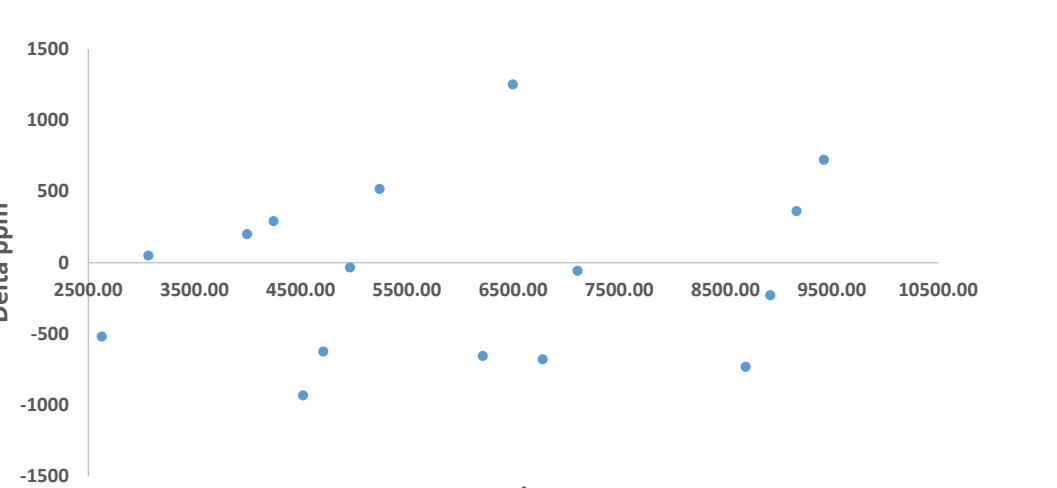
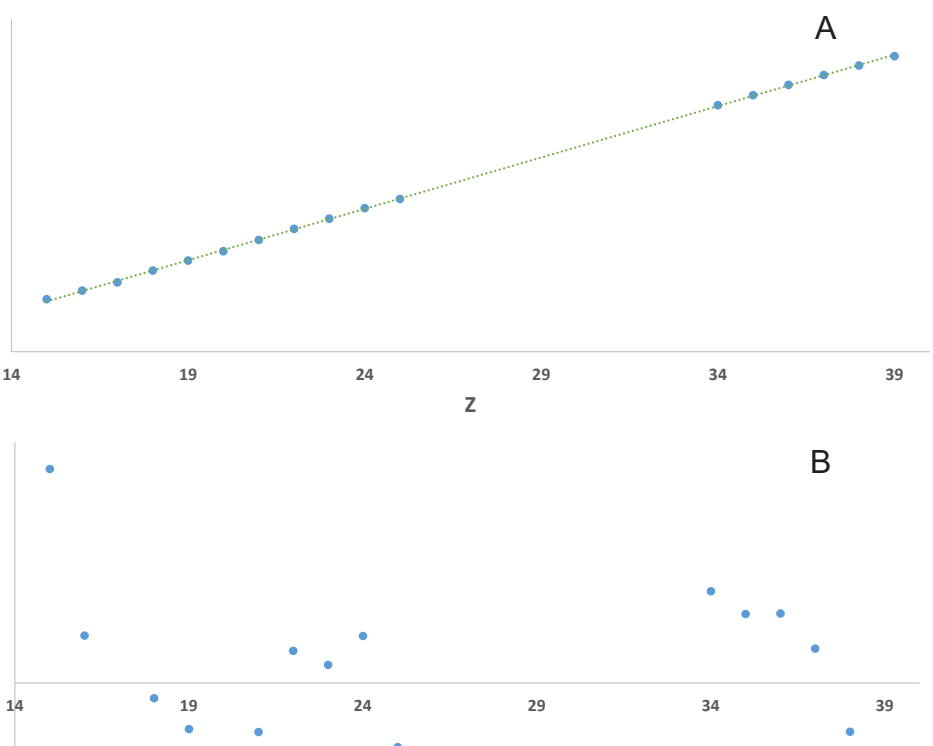


Figure 4.  $m/z$  residuals for calibrant peaks following calibration of the CDMS1 instrument. The RMS  $m/z$  error is 593 ppm.

Following  $m/z$  calibration, representative magnitudes were extracted for each charge state, allowing construction of a charge state calibration. The resulting linear calibration (see Eq. (1)) and associated residuals for the CDMS2 instrument are shown in Figure 5. The RMS charge residual is 0.093 elementary charges, demonstrating excellent linearity of charge measurement over the range of the calibrants. The intercept is  $-0.62$  charges, further indicating near proportionality.



## DISCUSSION

We have demonstrated a novel and robust approach to  $m/z$  calibration of MS data which is applicable when the masses of some calibrants are uncertain but bounded below by a minimum mass.

We achieve an  $m/z$  calibration of a novel Electrostatic Ion Trap CDMS instrument using five protein standards with an RMS of  $\sim 600$  ppm.

Calibration of two identical prototype instruments yielded calibrations that agree within 0.4% suggesting highly reproducible instrument construction.

Charge calibration of the instrument has also been demonstrated, showing near proportionality between number of charges and FFT magnitude and an RMS of less than 0.1 elementary charges.

Despite the availability of relatively mass-homogenous calibrants such as BLG